Eur Respir J 2012; 39: 446–457
DOI: 10.1183/09031936.00005511

Rescue of murine silica-induced lung injury and fibrosis by human embryonic stem cells

P. Spitalieri*, M.C. Quitadamo*, A. Orlandi*, L. Guerra#, E. Giardina*, V. Casavola#, G. Novelli*, C. Saltini¶ and F. Sangiuolo*

ABSTRACT: Alveolar type II pneumocytes (ATII cells) are considered putative alveolar stem cells. Since no treatment is available to repair damaged epithelium and prevent lung fibrosis, novel approaches to induce regeneration of injured alveolar epithelium are desired.

The objective of this study was to assess both the capacity of human embryonic stem cells (HUES-3) to differentiate *in vitro* into ATII cells and the ability of committed HUES-3 cells (HUES-3-ATII cells) to recover *in vivo* a pulmonary fibrosis model obtained by silica-induced damage.

***In vitro* differentiated HUES-3-ATII cells displayed an alveolar phenotype characterised by multilamellar body and tight junction formation, by the expression of specific markers such as surfactant protein (SP)-B, SP-C and zonula occludens (ZO)-1 and the activity of cystic fibrosis transmembrane conductance regulator-mediated chloride ion transport.**

After transplantation of HUES-3-ATII cells into silica-damaged mice, histological and biomolecular analyses revealed a significant reduction of inflammation and fibrosis markers along with lung function improvement, weight recovery and increased survival. The persistence of human SP-C, human nuclear antigen and human DNA in the engrafted lungs indicates that differentiated cells remained engrafted up to 10 weeks.

In conclusion, cell therapy using HUES-3 cells may be considered a promising approach to lung injury repair.

KEYWORDS: Cell therapy, human embryonic stem cells, lung fibrosis, silica damage

The pulmonary alveolar epithelium is an endoderm-derived tissue composed of two main cell populations: the alveolar type I (ATI) and type II (ATII) pneumocytes [1]. In addition, resident lung multipotent stem cells have been recently identified in the distal airways [2]. Besides characterising their phenotype and functional properties *in vitro* and *in vivo*, KAJSTURA *et al*. [2] described the capacity of these cells to give rise to different populations of endodermal epithelial cells and to pulmonary vessels. However, their capacity to promote tissue restoration in patients with lung disease has not yet been demonstrated. As the lung is constantly exposed to environmental toxicants and pathogens capable of injuring and destroying ATI cells on the alveolar surface, possibly leading to tissue destruction, lung structure distortion and respiratory dysfunction, ATII cells play a key role in lung homeostasis by producing surfactant proteins (SPs) and by their ability to undergo proliferation and differentiation to replace ATI cells [3]. Thus, the *in vitro* generation of ATII cells, capable of repairing damaged alveolar units [4], is likely to be instrumental to the treatment of lung diseases characterised by aberrant tissue remodelling, such as pulmonary fibrosis, where no effective drug is available and lung transplantation is the only treatment option. Exposure to crystalline silica may cause lung tissue reactions leading to both acute and chronic pulmonary disease manifestations ranging from nodular to massive forms of pulmonary fibrosis [5, 6]. As silica-induced tissue reactions can be reproduced in the mouse, where inhalation of silica causes lung inflammation and fibrosis [7], this study was designed to assess the ability of human embryonic stem cells (hESCs; cell line HUES-3) to differentiate into functioning ATII cells and to engraft into the lungs of mice with silica-induced

For editorial comments, see page 240.

AFFILIATIONS
*Depts of Biopathology, ¶Internal Medicine, Tor Vergata University of Rome, Rome, and #Dept of General Environmental Physiology, Bari University, Bari, Italy.

CORRESPONDENCE
F. Sangiuolo
Dept of Biopathology
Tor Vergata University of Rome
via Montpellier 131
00133 Rome
Italy
E-mail: sangiuolo@med.uniroma2.it

Received:
Jan 13 2011
Accepted after revision:
June 20 2011
First published online:
June 30 2011

European Respiratory Journal
Print ISSN 0903-1936
Online ISSN 1399-3003

pulmonary fibrosis in order to repair lung damage, mitigate pulmonary fibrosis and reduce mortality.

METHODS

Cell culture

HUES-3 cells (karyotype 46,XY) were propagated in undifferentiated embryonic stem cell medium (unESCM) [8]. For *in vitro* differentiation, cells were cultured in suspension in embryoid body (EB) medium (HUES-3 medium and activin A; R&D Systems, Inc., Minneapolis, MN, USA). EBs were cultured in adhesion in KnockOut Dulbecco's modified Eagle medium (KO-DMEM; Gibco, Invitrogen Corporation, Carlsbad, CA, USA) with 20% fetal bovine serum (FBS) for 10 days, and afterwards in small airway growth medium (SAGM; Clonetics, Milan, Italy) for 3, 5 and 8 days. Cells cultured without SAGM were used as controls [4]. This study on hESCs was approved by the Bioethical Committee of the Tor Vergata University Hospital (Rome, Italy).

Immunostaining

Cells were fixed in 4% paraformaldehyde and stained with antibodies against human pro-SP-C (1:2,000; Chemicon, Temecula, CA, USA) [4], human aquaporin (AQP)5 protein (1:50; Calbiochem, Merck, Darmstadt, Germany) [9], human tight junction protein zonula occludens (ZO)-1 (fluorescein isothiocyanate (FITC) conjugated; 1:50; Zymed Laboratories, San Francisco, CA, USA) [10], human cystic fibrosis transmembrane conductance regulator (CFTR; 1:500; Abcam, Cambridge, UK) [11] and human nuclear antigen (HuNu; 1:100; Chemicon) [12].

Real-time RT-PCR

Quantitative real-time RT-PCR was performed according to the manufacturer's protocol (Applied Biosystems, Monza, Italy) for SP-B and SP-C (SP-C117/134) [4], for the stem cell markers octamer-binding transcription factor (OCT)-4 (isoforms OCT-4A and OCT-4B), NANOG, CXC chemokine receptor (CXCR)4 and collagen type 1 α1 (Col1α1), for the inflammatory markers tumour necrosis factor (TNF)-α, monocyte inflammatory protein (MIP)-2 and interleukin (IL)-6, and for glyceraldehyde-3-phosphate dehydrogenase, which was used as a housekeeping gene as it is stable in differentiating embryonic stem cell cultures. Oligonucleotide sequences are shown in table 1.

TABLE 1 Oligonucleotides used in real-time PCR assays

	Forward	Reverse
hCXCR4	CTGTGAGCAGAGGGTCCAG	ATGAATGTCCACCTCGCTTT
hSP-C117	AGTGGAGCCGATGGAGAAG	GCAAAGAGGTCCTGATGG
hSP-C134	AGCCAGAAACACACGGAGAT	AGTGGAGCCGATGGAGAAG
hSP-B	ATGGTGAAACCCCATTTCTA	CAATTGATCAGTTAGGGTGG
hOCT-4A	CTCCTGGAGGGCCAGGAATC	CCACATCGGCCTGTGTATAT
hOCT-4B	ATGCATGAGTCAGTGAACAG	CCACATCGGCCTGTGTATAT
hNANOG	CAAAGGCAAACAACCCACTT	TCTGCTGGAGGCTGAGGTAT
hGAPDH	CAAATTCCATGGCACCGTCAA	CGCTCCTGGAAGATGGTGATG
mTNF-α	TCTCAAAATTCGAGTGACAAGC	ACTCCAGCTGCTCCTCCAC
mIL-6	GTTCTCTGGGAAATCGTGGA	TTCTGCAAGTGCATCATCGT
mMIP-2	GCGCCCAGACAGAAGTCATAG	GGCAAACTTTTTGACCGCC
mCol1α1	TCAGAGGCGAAGGCAACAGT	CCCAAGTTCCGGTGTGA
mGAPDH	ATGACATCAAGAAGGTGGTG	CATACCAGGAAATGAGCTTG

h: human; CXCR: CXC chemokine receptor; SP: surfactant protein; OCT: octamer-binding transcription factor; GAPDH: glyceraldehyde-3-phosphate dehydrogenase; m: murine; TNF: tumour necrosis factor; IL: interleukin; MIP: monocyte inflammatory protein; Col1α1: collagen type 1 α1.

Flow cytometry analysis

HUES-3-ATII cells, after 3, 5 and 8 days of culture with SAGM, were analysed after disaggregation by flow cytometry shortly after collection. Antibodies directed specifically against human stage-specific embryonic antigen (SSEA)-4 (2 μg·mL^{-1}; Chemicon), thyroid transcription factor (TTF)1 (1:30; GeneTex, Inc., San Antonio, TX, USA), CD105 (Endoglin; 1:20; BD Pharmingen, Franklin Lakes, NJ, USA) and CD34 (1:20; BD Pharmingen) were used according to the manufacturers' protocols.

Cytofluorimetric analyses were performed using a FACSCalibur flow cytometer (Becton-Dickinson, Franklin Lakes, NJ, USA) and resulting data were analysed using CellQuest software (Becton-Dickinson).

Fluorescence measurements of apical chloride efflux

Chloride efflux was measured using the chloride-sensitive dye MQAE in cells grown at confluence [13]. Fluorescence was recorded with a Cary Eclipse Spectrofluorometer (Varian, Palo Alto, CA, USA). CFTR-dependent chloride secretion was calculated as the difference in fluorescence stimulated by forskolin plus 3-isobutyl-1-methylxanthine with or without the specific CFTR inhibitor, $CFTR_{inh}$-172 [14].

Measurement of transepithelial electrical resistance

Transepithelial electrical resistance values were measured with a Millicell-ERS Volt Ohm Meter (Millipore, Billerica, MA, USA). All measurements were performed in triplicate and transepithelial electrical resistance values were normalised for the area of the filter and obtained after background subtraction.

Animals and experimental groups

A total of 160 female nude mice aged 8–9 weeks (Charles River, Wilmington, MA, USA) were used. They were divided into a group of 50 mice treated with saline solution and a group of 110 mice treated with silica. Experiments were conducted three consecutive times on different animals. Animal body weight was recorded daily. 10 more mice were used for teratoma formation.

Animal care was carried out in accordance with European Economic Community Council Directive 86/109, OJL 358, Dec 1 1987 and with the National Institutes of Health (Bethesda, MD, USA) Guide for the Care and Use of Laboratory Animals.

Silica treatment

Crystalline silica oxide powder (99.9%; Alfa Aesar, a Johnson Matthey Company, Karlsruhe, Germany) was administered intranasally at a concentration of 5 mg·mL^{-1} (50 μL·mouse^{-1}·day^{-1}) for 15 days. Control animals were sham treated with saline (50 μL·mouse^{-1}·day^{-1}) for 15 days.

HUES-3-ATII cell transplantation into nude mice

Silica-exposed mice were further subdivided into three groups: the ''silica+cells'' group, comprising 50 animals receiving 2.5×10^6 cells by intratracheal instillation after 15 days of silica treatment; the ''silica'' group, comprising 50 animals receiving

silica treatment for 15 days but no cells; and a group of 10 silica-damaged animals that were inoculated intratracheally with 2.5×10^6 human fibroblasts. HUES-3-ATII cells were injected after 3 days of SAGM treatment.

In addition, a group of 10 animals were injected subcutaneously with 2.5×10^6 HUES-3-ATII cells and sacrificed after 3 months to evaluate teratogenicity.

Real-time RT-PCR detection of murine/human chimerism

Human DNA was detected in the mouse lungs using probes for the hTERT locus (Quantifiler kit; Applied Biosystems, Carlsbad, CA, USA) for the quantification of human nuclear DNA [15] and/or probes for human cytochrome B [16]. Quantifiler data analysis was performed using the SDS software (SDS Software, Vancouver, BC, Canada) to generate standard curve data for quantification standards and results for unknown samples.

Histological examination

Both silica and silica+cells groups were sacrificed for histological evaluation 5, 10 and 15 days after cell administration. Serial sections from formalin-fixed multiple slices of constant thickness [17] were stained with haematoxylin and eosin and Masson's trichrome to evaluate the extent of lung inflammation and the severity of fibrosis according to the method of ASHCROFT *et al*. [18], respectively.

Transmission electron microscopy

Cells were post-fixed in 1% OsO_4 for 2 h and dehydrated through an alcohol series and propylene oxide before embedding in EPON 812 (Shell Chemical Corp., Cleveland, OH, USA). Thin sections were stained with toluidine blue and ultrathin sections were cut by an 8800 ultramicrotome III (LKB Instrument, Dübendorf, Switzerland), counterstained with uranyl acetate and lead citrate and analysed by a Philips Morgagni electron microscope (Morgagni^{TM} 268; FEI Company, Hillsboro, OR, USA).

Protein analysis

Proteins were extracted from mouse lung using RIPA (radioimmunoprecipitation assay) buffer according to the manufacturer's instructions (Sigma–Aldrich, Milan, Italy), and analysed by Bio-Rad dye-binding protein assay (Bio-Rad, Berkeley, CA, USA).

Antibodies for transforming growth factor (TGF)-β (1:200; Santa Cruz Biotechnology, Santa Cruz, CA, USA), Col1α1 (1:10000; Abcam) and β-actin (1:5000; Santa Cruz Biotchnology) were used as reported [19, 20]. The ECL Advanced detection

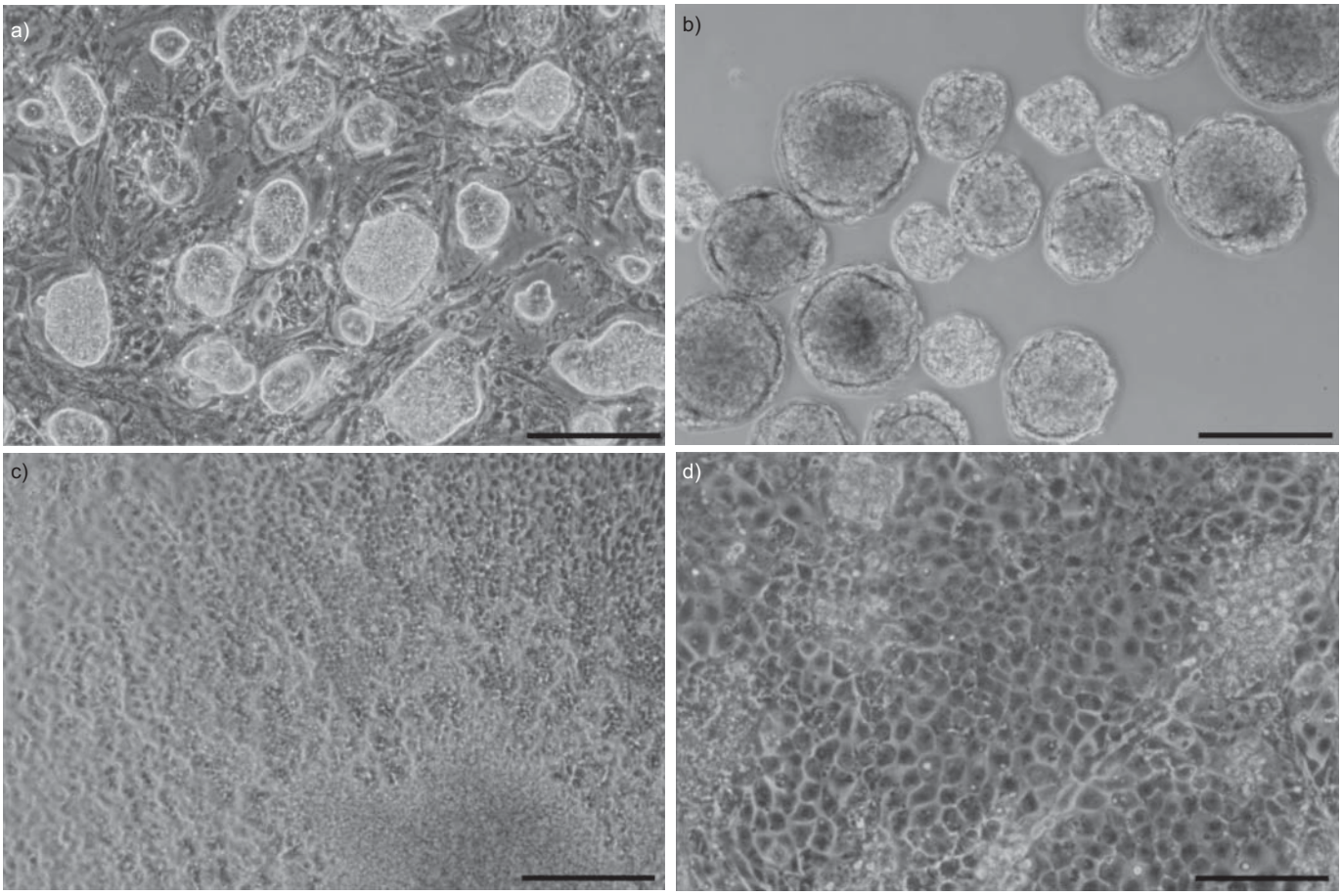

FIGURE 1. a) HUES-3 cells on a murine embryonic fibroblast feeder layer. b) Embryoid bodies (EBs) treated with activin A (10 ng·mL^{-1}) after 6 days of cell culture. c) EBs in adhesion after 10 days. d) EBs treated with small airway growth medium for 8 days. Scale bars: a–c) 200 μm; d) 100 μm.

kit (Amersham Pharmacia Biotech Ltd, Piscataway, NJ, USA) was used according to the manufacturer's instructions.

Oxygen saturation

Blood arterial oxygen saturation was recorded using a small rodent oximeter sensor mounted on the thigh of each experimental animal (MouseOX; STARR Life Sciences, Oakmont, PA, USA). Three groups of animals were recorded, each containing five mice. Data were collected for a minimum of 10 s without any error code and the measurement was repeated six times within a 3-min period.

Statistical analysis

Data were expressed as mean±SEM for multiple independent experiments, as indicated. For statistical analysis the unpaired t-test was used. A p-value <0.05 was regarded as significant.

RESULTS

In vitro *differentiation of HUES-3 into ATII cells*

HUES-3 cell colonies were cultured on a murine fibroblast layer (fig. 1a), then were detached from the feeder layer and differentiated in suspension to form fairly regular EBs (fig. 1b), which could in turn form an endodermal layer when treated with activin A. EBs, when transferred into adherent culture conditions, displayed an epithelial-like phenotype (fig. 1c) and differentiated into ATII epithelial cells after 8 days in SAGM culture (fig. 1d) [4]. This was shown after 8 days of culture in SAGM by immunocytochemistry with confocal microscopy using anti-SP-C (an ATII cell phenotype marker) and anti-AQP5 (an ATI cell phenotype marker) antibodies, as differentiated HUES-3 cells expressed SP-C (fig. 2a) but not AQP5 (fig. 2e). In addition, they expressed the ZO-1 protein, a tight junction marker characteristic of epithelial structures (fig. 2c).

As expected, real-time RT-PCR of stem cell markers revealed a decrease of OCT-4 (isoforms A and B) and NANOG from day 5 of differentiation (fig. 3a). Also, flow cytometric analysis of the SSEA-4 protein revealed a gradual reduction from day 3 to day 8 of differentiation (from mean±SEM 14±0.03% to 6.7±0.01%; fig. 3b). Differentiated cells revealed a cell population positive for TTF-1 (mean±SEM 94.8±0.02%; fig. 3e), a marker selectively expressed in ATII cells, and only 2% of cells positive for CD105 (a mesenchymal cell marker; fig. 3c) and CD34 (an endothelial cell marker; fig. 3d). Furthermore, the expression of transcripts from SP-C isoforms and of SP-B progressively increased during differentiation in SAGM, with respect to the control cells not receiving SAGM (fig. 3f). Chemokine receptor CXCR4 [21] expression also markedly increased as soon as the cells started their differentiation treatment with SAGM (fig. 3g).

In addition, two typical epithelial features, the ATII cell intracytoplasmic lamellar bodies in which SP-C is stored (fig. 4a and b) and the epithelial intercellular junctions (fig. 4c), could be shown by transmission electron microscopy in HUES-3-ATII cells after 5 days of SAGM culture.

CFTR expression and activity in HUES-3-ATII cells

Confocal analysis of CFTR expression in HUES-3 cells grown with or without adding SAGM in the cell medium showed heightened expression of the CFTR protein [22] on the apical membrane of HUES-3 cells after 5 days in SAGM (fig. 5a), compared with low and random expression on untreated cells. Details of CFTR immunohistochemical analysis are reported in figure 5e, where a three-dimensional view of a single cell was cropped from a confocal z-stack acquisition. Consistent with the above observations, HUES-3-ATII cells, grown to confluence on permeable supports coated with Cultrex® Basement Membrane

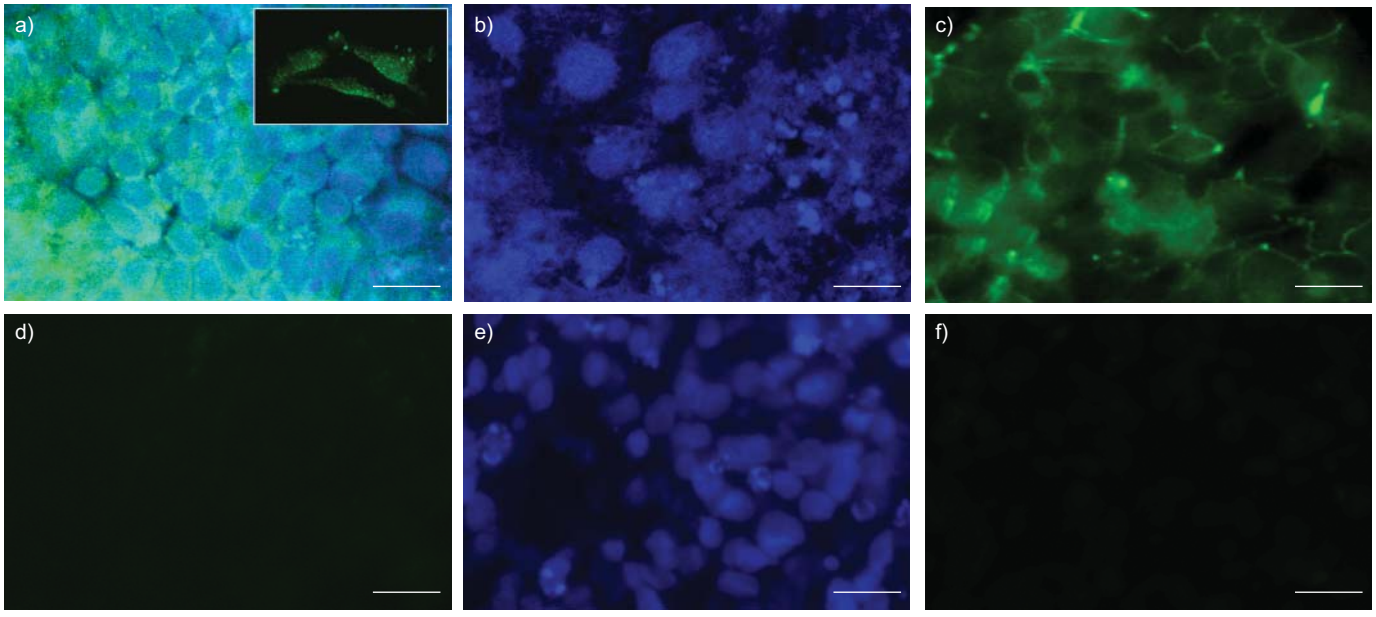

FIGURE 2. a) Confocal analysis of human surfactant protein (SP)-C antibody (green) localised on membranes of HUES-3 alveolar type II (ATII) cells after 8 days of small airway growth medium (SAGM) treatment. Inset shows a three-dimensional view; cells were cropped from a confocal z-stack acquisition. b) Cells not treated with SAGM did not show staining for SP-C. c) HUES-3-ATII cells, grown for 8 days in SAGM, showed an immunoreactivity for the tight junction marker zonula occludens (ZO)-1 (green). d) Cells not treated with SAGM did not show staining for ZO-1. e) HUES-3-ATII cells grown for 8 days in SAGM and f) cells not treated with SAGM did not show any signal for aquaporin (AQP)5 protein. Nuclei stained with TO PRO 3 (blue). Scale bars: 20 μm.

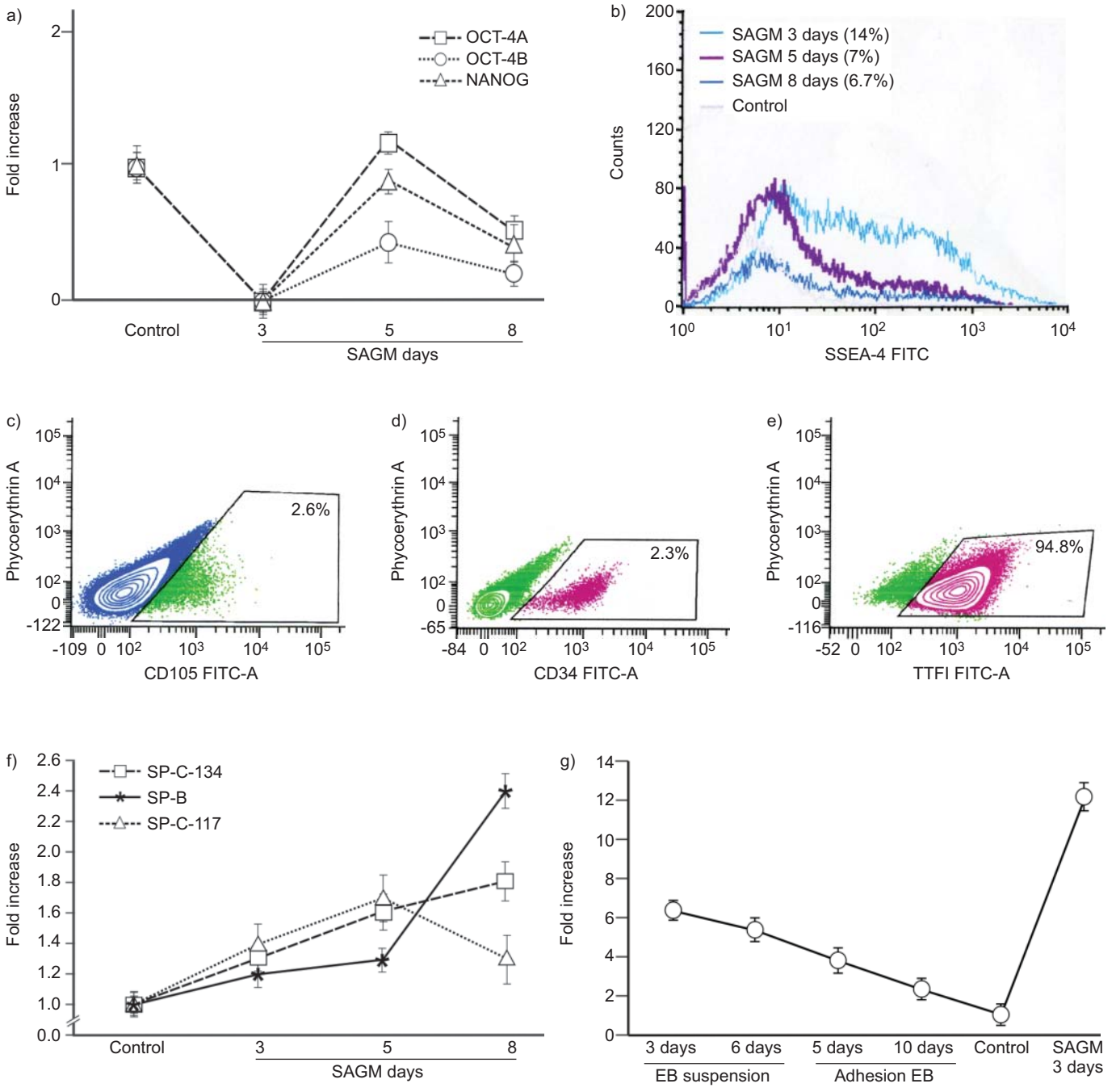

FIGURE 3. a) Quantification of octamer-binding transcription factor (OCT)-4, isoforms A and B, and NANOG transcripts in control cells (no small airway growth medium (SAGM)) and in HUES-3 alveolar type II (ATII) cells after 3, 5 and 8 days of SAGM. The fold increase of each transcript is calculated compared with control cells: $p \leqslant 0.05$ after 3 days, $p \leqslant 0.02$ after 5 days and $p \leqslant 0.04$ after 8 days for OCT-4; $p \leqslant 0.01$ after 3 days, $p \leqslant 0.02$ after 5 days and $p \leqslant 0.03$ after 8 days for NANOG. All values obtained are the mean of at least three independent experiments performed in triplicate. b) Fluorescence-activated cell sorting (FACS) analysis using fluorescein isothiocyanate (FITC)-conjugated stage-specific embryonic antigen (SSEA)-4 stem cell marker on HUES-3-ATII cells after 3, 5 and 8 days of SAGM. The control is the isotype control. c–e) FACS analysis of HUES-3-ATII cells using FITC-conjugated c) monoclonal CD105 antibody (a mesenchymal stem cell marker), d) CD34 antibody (an endothelial marker) and e) thyroid transcription factor (TTF)1 rabbit monoclonal antibody (for type II epithelial cells), after 3 days of SAGM. The data indicated a mean$\pm$SEM of c) $2.6 \pm 0.01\%$, d) $2.3 \pm 0.01\%$ and e) $94.8 \pm 0.02\%$ of cells positive within the differentiated cell population. f) Surfactant protein (SP)-B and SP-C (117 and 134 isoforms) expression in HUES-3-ATII cells after 3, 5 and 8 days of SAGM. The fold increase of each transcript is calculated compared with control cells (no SAGM): $p \leqslant 0.02$ after 3 days, $p \leqslant 0.03$ after 5 days and $p \leqslant 0.05$ after 8 days for SP-B; $p \leqslant 0.01$ after 3 days, $p \leqslant 0.03$ after 5 days and $p \leqslant 0.04$ after 8 days for SP-C-117, $p \leqslant 0.05$ after 3 days, $p \leqslant 0.02$ after 5 days and $p \leqslant 0.04$ after 8 days for SP-C-134. g) Quantitative analysis of CXC chemokine receptor (CXCR)4 expression from embryoid bodies (EBs), from formation to their adhesion and until 3 days of SAGM treatment. The fold increase of each transcript is calculated compared with control cells (no SAGM): $p \leqslant 0.01$ for cells after 3 days with SAGM.

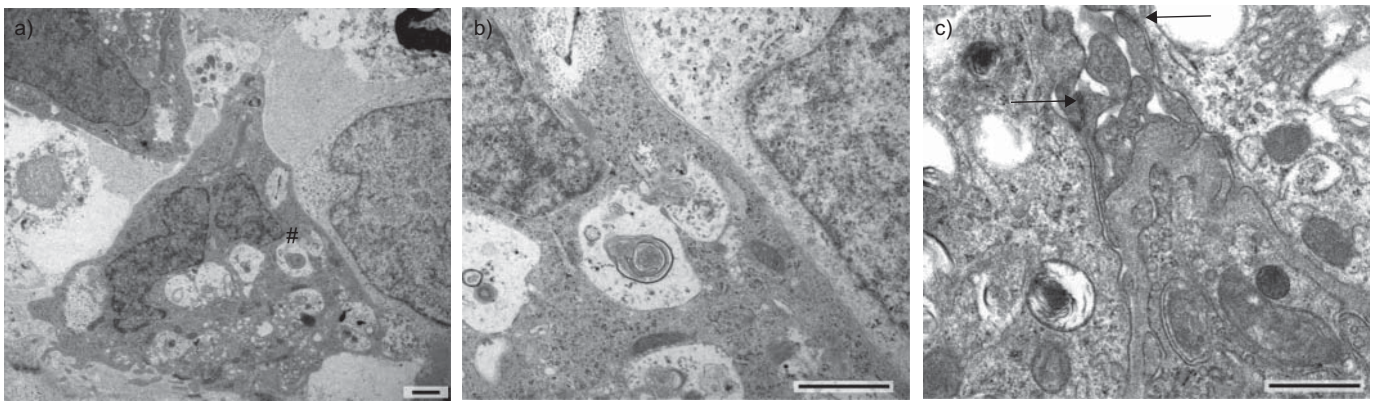

FIGURE 4. a) Transmission electron microscopy of HUES-3 alveolar type II (ATII) cells after 5 days of small airway growth medium *in vitro*. The bubble-like appearance and the presence of intracytoplasmic lamellar body organelles (#) indicate typical ultrastructural features of ATII cells. b) At higher magnification, details of an intracytoplasmic lamellar body. c) Higher magnification showing the presence of well-defined epithelial cell contacts including tight junctions (arrows) Scale bars: 2 μm.

Extract (Corning Inc., Lowell, MA, USA), displayed significantly increased transepithelial electrical resistance, indicating differentiation toward the ATII cell phenotype (table 2). Similarly, HUES-3-ATII cells after 3 and 5 days in SAGM culture showed significantly increased CFTR-dependent chloride efflux when compared with control untreated cells (fig. 5f), as measured by fluorescence analysis with the chloride-sensitive dye MQAE after chloride/nitrate substitution in the apical perfusion medium (fig. 5g) [11].

Microscopic and molecular analyses of lung parenchymal damage before and after HUES-3-ATII cell injection

After crystalline silica instillation, inflammatory infiltrates composed of foamy cells, lymphocytes and neutrophils became progressively more widespread (fig. 6a and b, silica groups), leading to progressive multifocal fibrosing alveolitis with a nodular peribronchiolar organisation [23].

Treatment with HUES-3-ATII cells significantly reduced inflammation and fibrosis in silica-instilled mice after 10 and 15 days from cells injection (fig. 6a and b, silica+cells groups), in comparison with control mice as shown by Ashcroft score analysis ($p<0.01$; fig. 6c).

The engraftment of human ATII cells into the mouse lungs was demonstrated in the lungs of HUES-3-ATII cell-treated mice 4 weeks after cell administration. Expression of HuNu (fig. 7a) and of human SP-C was shown by immunohistochemistry to colocalise in ATII cells (fig. 7b). Molecular analysis revealed the presence of human DNA in the same tissue samples (fig. 7d). The engraftment of human alveolar cells within murine lungs was confirmed by confocal microscopy on ATII cell-treated mice up to 10 weeks after cell transplantation (fig. 7c). Furthermore, teratogenicity of transplanted HUES-3-ATII cells was ruled out by histological examination 1 yr after HUES-3-ATII cell injection in nude mice (data not shown).

Assessment of recovery of lung damage and fibrosis in HUES-3-ATII cell-transplanted mice

Silica-induced lung damage and fibrosis were also evaluated by monitoring the expression of TGF-β protein during silica exposure (silica groups after 5, 10 and 20 days) as well as 20 days after HUES-3-ATII cell administration (silica+cells group after 20 days; fig. 8a). As reported by densitometric analysis, an increase of TGF-β, indicative of a fibrosis onset, was detected during silica exposure. Conversely, administration of HUES-3-ATII cells resulted in a marked reduction of TGF-β expression *in vivo* compared with mice not receiving cells (silica+cells *versus* silica group after 20 days; fig. 8a). No reduction was seen when fibroblast cells were injected instead of HUES-3-ATII cells. A similar pattern was obtained for Col1α1, indicative of fibrosis onset. Collagen expression was markedly reduced only when HUES-3-ATII cells were injected (silica+cells group after 20 days) and not when fibroblast cells were used (fig. 8b). In addition, the expression of the pro-inflammatory mediators IL-6, TNF-α and MIP-2 was clearly reduced after HUES-3-ATII cell injection (silica+cells group) if compared with silica-injured (silica group) at each time-point (5, 10 and 15 days; fig. 8d). No reduction was found in silica-injured mice injected with fibroblast cells (silica+fib group). Consistent with pro-inflammatory and pro-fibrotic cytokine expression, the level of the collagen deposition marker Col1α1 showed a five-fold increase in silica-exposed mice at 15 days, with a significant reduction after HUES-3-ATII cell administration. Quantitative values were normalised with respect to those obtained in control mice injected with saline solution (fig. 8d).

Consistent with the observed reduction of inflammation and fibrosis, HUES-3-ATII cell treatment also resulted in a marked improvement of lung function. Importantly, HUES-3-ATII cell-treated mice showed, in comparison with silica-damaged mice, a marked improvement of blood oxygenation, as their saturation values remained in the range of silica-unexposed control mice (fig. 8c).

Finally, HUES-3-ATII cell administration to silica-exposed mice resulted in an evident improved survival (fig. 8e). While weight loss progressed from the first day of damage in silica-instilled mice not receiving HUES-3-ATII cells, a striking 95% recovery of pre-treatment weight was observed in mice 20 days after HUES-3-ATII cell treatment (fig. 8e). Mice not receiving cells, or receiving fibroblasts, progressively died with an observed 100% mortality.

Confirming the specific effect of hESC treatment in ameliorating silica-induced lung injury and fibrosis, silica-injured mice

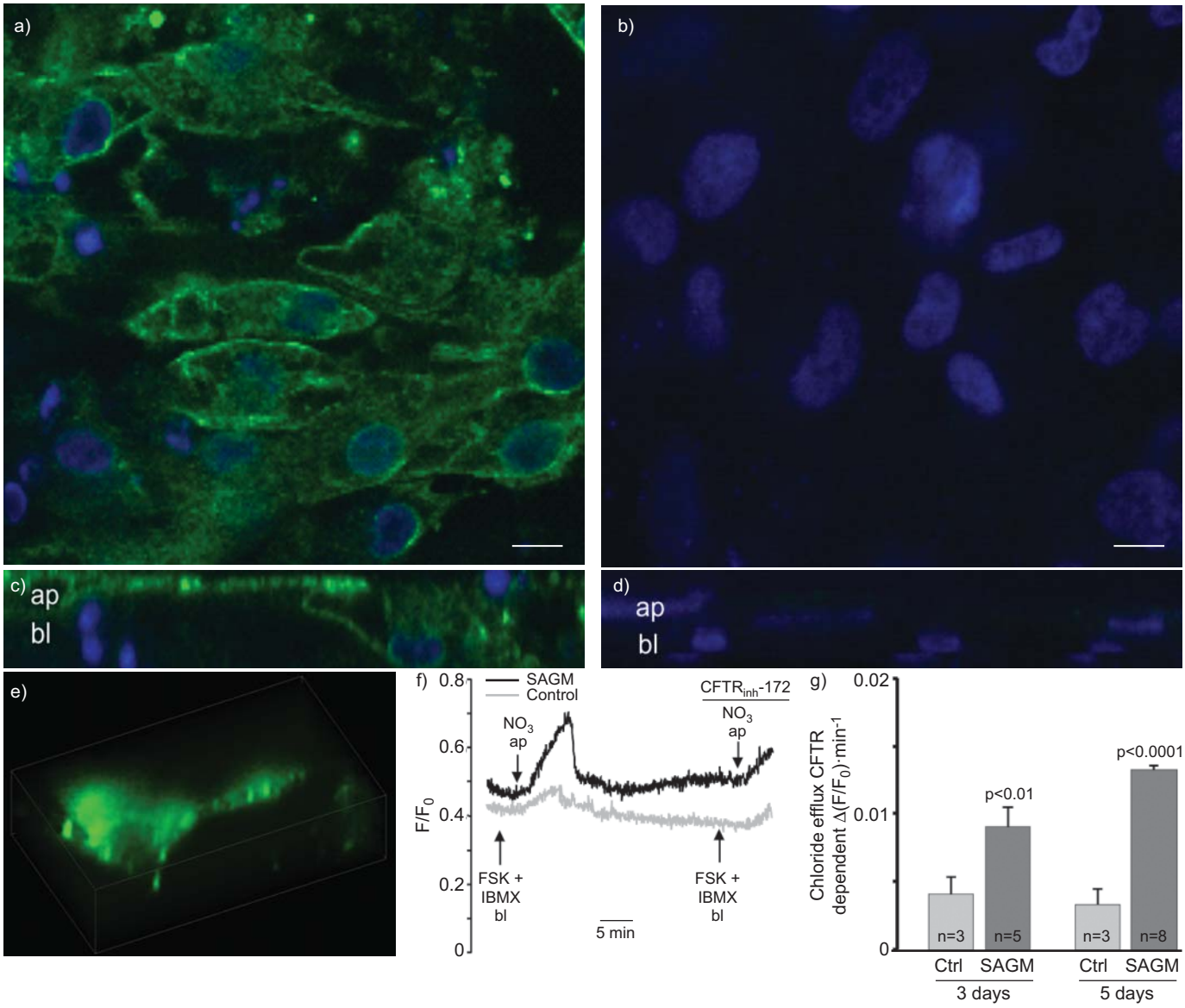

FIGURE 5. a–d) Confocal immunofluorescence microscopy was performed in (a and c) HUES-3 alveolar type II (ATII) cells after 5 days treatment with small airway growth medium (SAGM) and in (b and d) untreated cells. Unpermeabilised cells were immunolabelled with a primary mouse monoclonal antibody (CF3) raised against the first loop of cystic fibrosis transmembrane conductance regulator (CFTR; green). a and b) The horizontal sections (xy) were taken at the apical region. c and d) The vertical sections (xz) were randomly acquired. ap: location of apical region; bl: location of basal region. e) Three-dimensional view of a single cell cropped from a confocal z-stack acquisition, showing the distribution of CFTR (green) in a differentiated HUES-3 cell. f) Typical recordings showing changes in intracellular chloride-dependent MQAE fluorescence in both SAGM-treated HUES-3-ATII cells and in untreated monolayers (control) in the absence or presence of the specific CFTR inhibitor, $CFTR_{inh}$-172 (5 μM). CFTR-dependent chloride secretion is calculated as the difference in the rate of change of forskolin (FSK) plus 3-isobutyl-1-methylxanthine (IBMX) stimulated fluorescence with or without $CFTR_{inh}$-172. NO_3: nitrate. g) Summary of the data collected from different experiments performed as in f) after 3 and 5 days of treatment. Statistical comparison was made using unpaired t-test with respect to the values obtained in control cells (Ctrl; no SAGM). Scale bars: 10 μm.

sham treated with human fibroblasts showed no change in either weight loss progression or death rates (data not shown).

DISCUSSION

Pulmonary fibrotic disorders, either idiopathic or associated with collagen vascular diseases or caused by environmental exposures, may lead to lung structure distortion and dysfunction with ensuing respiratory failure. For the most severe fibrotic disorder, idiopathic pulmonary fibrosis (IPF)/usual interstitial pneumonia, no medical treatment has been shown so far to be capable of arresting or reversing lung damage and fibrosis [24].

Bleomycin-induced lung inflammation and fibrosis in mice have been widely used as the most reliable model of pulmonary fibrosis, IPF in particular [25], and a number of studies have been carried out to attempt to restore lung structure and function using stem cell transplant in bleomycin-treated mice. These studies showed that stem cell treatment can reduce inflammation and fibrosis while restoring alveolar structures in bleomycin-induced pulmonary fibrosis [26–29]. Other strategies have been explored for the repair and regeneration of the injured lung. Intratracheal instillation of palifermin (DN23-KGF), a recombinant keratinocyte growth factor (KGF), has been

TABLE 2 Summary of measurements of transepithelial electrical resistance

Days after EB adhesion and expansion on insert	Days after differentiation in SAGM	Transepithelial electrical resistance $\Omega \cdot cm^2$	Experiments n
8	0	163.83±3.83	18
11	3	184.83±5.67**	5
13	5	204.71±5.80$^{\#}$	8

Data are expressed as mean±SEM, unless otherwise stated. EB: embryoid body; SAGM: small airway growth medium. **: $p<0.01$; $^{\#}$: $p<0.0001$; using unpaired t-test with respect to the values obtained in cells not treated with SAGM.

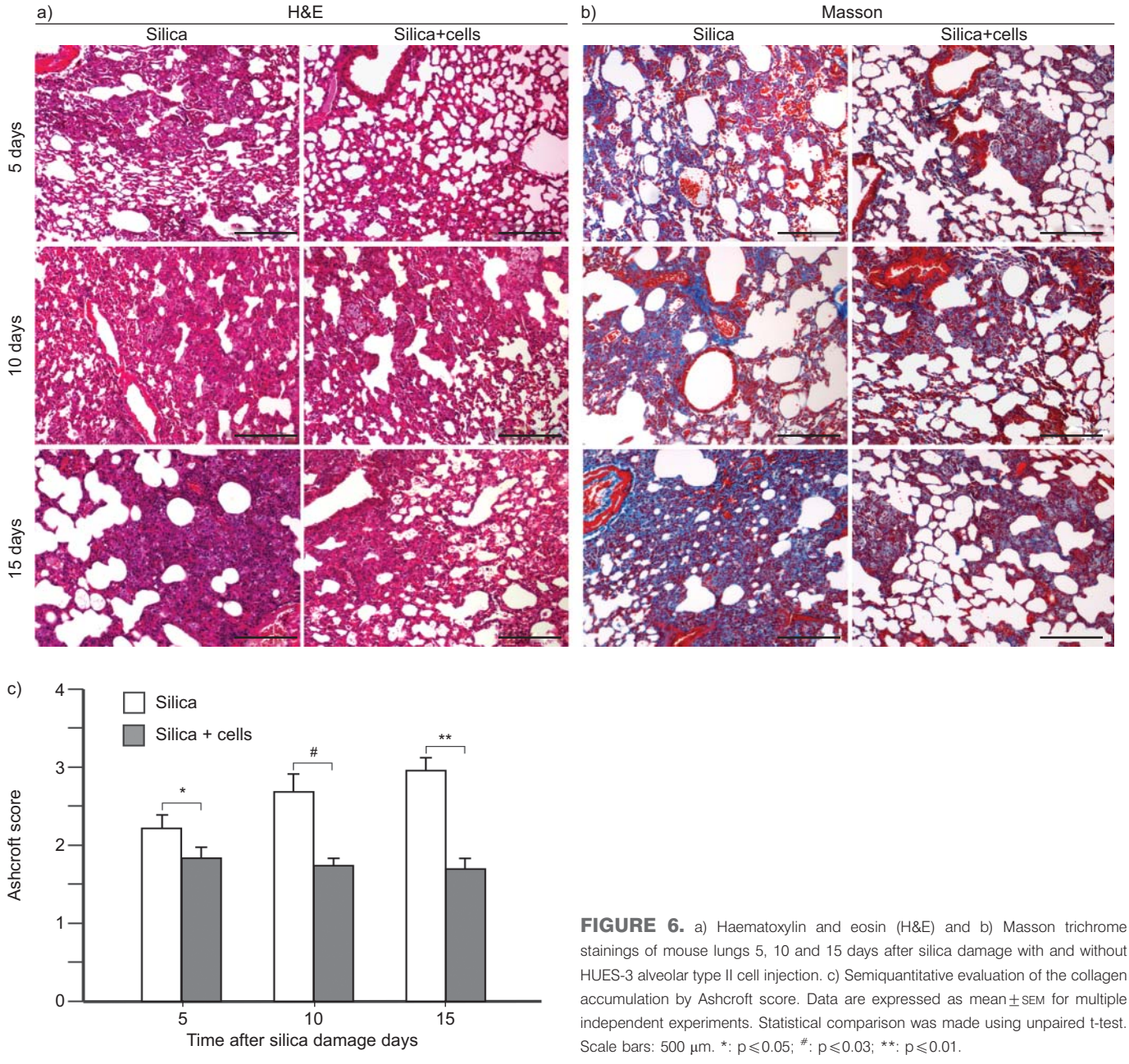

FIGURE 6. a) Haematoxylin and eosin (H&E) and b) Masson trichrome stainings of mouse lungs 5, 10 and 15 days after silica damage with and without HUES-3 alveolar type II cell injection. c) Semiquantitative evaluation of the collagen accumulation by Ashcroft score. Data are expressed as mean±SEM for multiple independent experiments. Statistical comparison was made using unpaired t-test. Scale bars: 500 μm. *: $p \leqslant 0.05$; $^{\#}$: $p \leqslant 0.03$; **: $p \leqslant 0.01$.

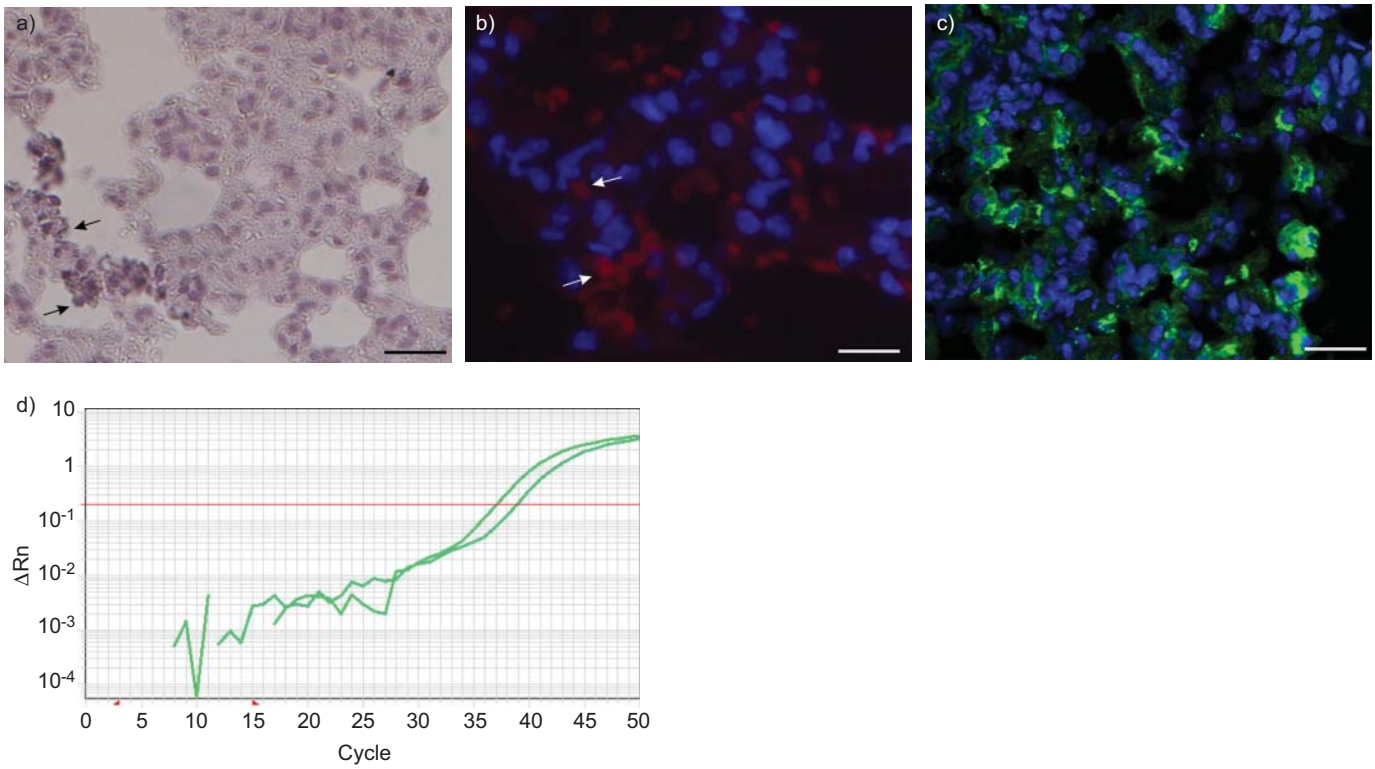

FIGURE 7. a) Immunostaining for human nuclear antigen (HuNu) was performed using the streptavidin-polyADP ribose polymerase (PARP) diaminobenzidine (DAB) peroxidase system on representative sections of silica-treated lung from HUES-3 alveolar type II (ATII) cell-injected mice. Arrows show positive cells. b) Subsequent section in which the same cells (arrows) were shown to be positive for human surfactant protein (SP)-C antibody (red) at higher magnification. c) Human SP-C hybridisation analysed by confocal microscopy on silica-treated lungs 10 weeks after cell transplantation. d) Detection of human DNA in silica-treated lungs from HUES-3-ATII cell-injected mice by the Quantifiler Human kit assay (Applied Biosystems, Carlsbad, CA, USA). A negative control performed on damaged mice in which no HUES-3-ATII cells were injected did not reveal any presence of human DNA (data not shown). ΔRn: change in normalised reporter signal. Red line: threshold of 0.2. Scale bars: a) 100 μm; b) 30 μm; c) 60 μm.

shown to be capable of stimulating emphysematous lung regeneration in experimental animals, probably through enhanced production of cytokines such as vascular endothelial growth factor and TGF-β [30]. Interestingly, transplantation of lentivirus-transduced bone marrow haemopoietic stem cells expressing KGF has been shown to attenuate lung damage in a bleomycin murine model of pulmonary fibrosis [31], possibly *via* complex paracrine interaction. Another epithelial cell growth factor, hepatocyte growth factor (HGF), has also been successfully used to treat bleomycin-induced pulmonary fibrosis by toracothomic lung administration of an HGF plasmid (pCikhHGF) using electroporation [32].

Other studies have been carried out using stem cell transplantation (either mesenchymal cells or cells derived from fetal membranes of human term placenta) in animal models in which lung fibrosis has been induced by bleomycin and also by silica [26, 33–36]. These cells were found to express alveolar epithelium markers after injection into mice and to exert significant anti-inflammatory and anti-fibrotic effects in the bleomycin as well as in the silica models of fibrosis. However, only one group [27] reported evidence that long-term engrafted cells could functionally differentiate into type II pneumocytes, by demonstrating secretion of SP-D expression following stimulation with corticosteroids. Bone marrow-derived cells, once instilled into silica-injured mice, allowed a transient beneficial effect until 2 months after cell administration. Similar paracrine effects were described using bone marrow-derived mononuclear cells, for which no engraftment was reported despite an evident improvement of lung function [35].

With regard to hESCs, their ability to differentiate into functional ATII cells has been shown in two studies [4, 28]. SAMADIKUCHAKSARAEI *et al*. [4] reported *in vitro* differentiation of hESCs into a mixed population of cells containing a small percentage of ATII cells, not suitable for transplantation because of the risk of producing teratomas after transplantation. WANG *et al*. [28] generated a stable transfected hESC line homogeneously expressing an ATII cell phenotype that, once transplanted in a mouse model of bleomycin-induced lung injury, was able to functionally repair the acutely injured alveolar epithelium, without causing teratoma formation.

To date, no study using hESCs has been described in silica-induced lung injury in an *in vivo* mouse model. The present study is, to our knowledge, the first reporting the use of *in vitro* differentiated hESCs for the treatment of silica-induced pulmonary fibrosis in the mouse model, and it shows that HUES-3 cells were capable of differentiating into ATII cells, grafting into the mouse lung, repairing lung injury and ameliorating disease course, rescuing mice from death.

First, after differentiation in culture, HUES-3 cells expressed the alveolar epithelial cell markers SP-C, ZO-1, CXCR4 and active CFTR, while downregulating the expression of the stem

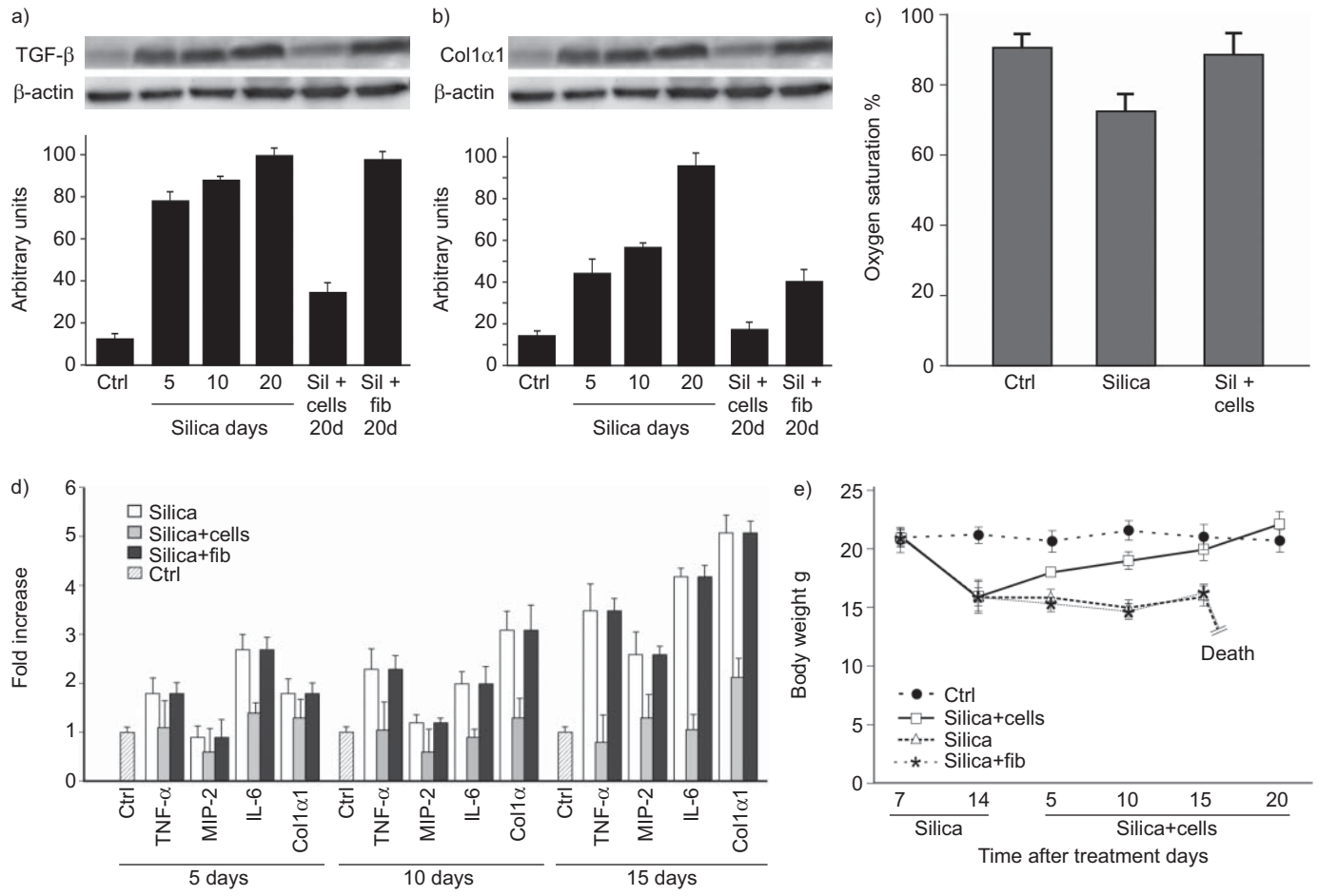

FIGURE 8. Western blot analysis for a) transforming growth factor (TGF)-β and b) collagen type 1 α1 (Col1α1) in lung tissue from control (Ctrl; undamaged mice), mice damaged after 5, 10 and 20 days of silica treatment and from mice 20 days after HUES-3 alveolar type II (ATII) cell (Sil+cells 20d) and fibroblast cell (Sil+fib 20d) injection. For both, densitometric analysis revealed a reduction in expression after HUES-3-ATII cell administration in damaged mice (sil+cells 20d). All values obtained are the mean of at least three independent experiments. Note that monomeric collagen type 1 consists of α1 (110 kDa) and α2 (135 kDa) chains. c) Blood arterial oxygen saturation levels were recorded on day 15 after silica damage (n=5) and showed a significant decrease when compared with control mice injected with saline solution (Ctrl; n=5). After HUES-3-ATII cell injection (silica+cells; n =5), a complete recovery of normal arterial oxygen saturation levels was recorded ($p<0.02$). d) Real-time RT-PCR analysis for inflammatory cytokines on silica- treated lungs. An evident reduction of cytokine expression was found after HUES-3-ATII cell injection (silica+cells groups) with respect to damaged mice (silica groups). After 5 days: tumour necrosis factor (TNF)-α $p<0.05$; monocyte inflammatory protein (MIP)-2 $p<0.02$; interleukin (IL)-6 $p\leqslant0.03$; Col1α1 $p\leqslant0.01$. After 10 days: TNF-α $p<0.03$; MIP-2 $p\leqslant0.01$; IL-6 $p\leqslant0.05$; Col1α1 $p\leqslant0.04$. After 15 days: TNF-α $p<0.05$; MIP-2 $p<0.01$; IL-6 $p\leqslant0.02$; Col1α1 $p\leqslant0.03$. No reductions were recorded in mice injected with fibroblast cells (silica+fib). The fold increase of each transcript is calculated compared with control mice injected with an equivalent volume of saline solution (Ctrl). All values obtained are the mean of at least three independent experiments performed in triplicate. e) Daily body weight measurement from the first day of silica treatment in damaged mice (silica), damaged and HUES-3-ATII cell-injected mice (silica+cells), damaged mice injected with fibroblast cells (silica+fib) and in control mice injected with saline solution (Ctrl). An evident body weight recovery was shown in silica+cells mice ($p<0.05$; n=10). Silica-damaged mice receiving fibroblasts or not receiving cells progressively died.

cell markers OCT-4, NANOG and SSEA-4, thus demonstrating that an ATII phenotype could be obtained [37, 38] through *in vitro* differentiation of HUES-3 cells.

Secondly, as it has been shown that the turnover of the adult mammalian alveolar epithelium is ~3–4 weeks [39], the observation that transplanted HUES-3-ATII cells could be identified in the lungs of silica-injured mice up to 10 weeks after cell administration suggests the engraftment of HUES-3-ATII cells after intrapulmonary injection.

Thirdly, the efficacy of intrapulmonary injection of HUES-3-ATII cells in the treatment of lung inflammation and fibrosis in silica-injured mice, an experimental condition known to cause 100% mortality within 3 weeks [40], was proven in both pathological and clinical terms. It is well known that the expression of inflammatory cytokines, in particular of IL-6, is significantly elevated in silica-induced experimental lung injury, where it may act in synergy with TNF-α and TGF-β to perpetuate inflammation and fibrosis [41–47], resulting in increased type I collagen deposition. In our study, the reduction of inflammatory changes at the tissue level was associated with a marked reduction of the expression of IL-6, TNF-α and MIP-2 shown only in mice receiving HUES-3-ATII cells but not in those receiving an equivalent volume of saline solution. Accordingly,

pulmonary function was preserved and survival of silica-exposed mice was significantly improved after HUES-3-ATII cell treatment.

The mechanism by which HUES-3-ATII cells repair lung damage and reverse fibrosis remains to be elucidated. It has been shown that ATII cells function as epithelial cell precursors in the alveoli during fetal development and early life and that they are capable of regaining their migratory and proliferative potential after lung injury and alveolar damage, such as in hyperoxic oxidative stress [48]. ATII cells are known to play a key role in the response to the exposure to toxic silica. ATII cell hyperplasia is seen in animal models as an early event following ATI cell epithelial damage [39] and it is a common finding in the lower respiratory tract of individuals with pulmonary silicosis [49]. In this context, experimental studies demonstrating that ATII epithelial cell disruption may lead to exaggerated fibrotic lung responses [50] are consistent with the hypothesis that failure of ATII cells to express their regenerative potential may play a role in the relentless progression of IPF [51].

The data presented here strongly support the possibility that differentiated stem cells such as the HUES-3-ATII cells, as they express CXCR4, may be capable of locating to the alveoli [52], where they can significantly reduce lung damage, type 1 collagen deposition and fibrotic tissue formation, and thus represent a potentially applicable tool for innovative anti-fibrotic, cell-mediated treatment [28, 53].

The results obtained in this silica-induced lung fibrosis model bring further support to the potential usefulness of this differentiated stem cell therapy, as the administration of HUES-3-ATII cells was both effective, reducing mortality of silica-injured mice, and safe, being devoid of teratogenic risks.

In conclusion, our results show that hESC transplantation effectively reduces silica-induced lung fibrosis in mice after intratracheal injection, indicating that the cell therapy approach may be a potentially useful strategy for the treatment of fibrotic lung diseases.

STATEMENT OF INTEREST

None declared.

REFERENCES

1 Mason RJ. Biology of alveolar type II cells. *Respirology* 2006; 11: Suppl., S12–S15.
2 Kajstura J, Rota M, Hall SR, *et al.* Evidence for human lung stem cells. *N Engl J Med* 2011; 364: 1795–1806.
3 Bishop AE. Pulmonary epithelial stem cells. *Cell Prolif* 2004; 37: 89–96.
4 Samadikuchaksaraei A, Cohen S, Isaac K, *et al.* Derivation of distal airway epithelium from human embryonic stem cells. *Tissue Eng* 2006; 12: 867–875.
5 Greenberg MI, Waksman J, Curtis J. Silicosis: a review. *Dis Mon* 2007; 53: 394–416.
6 Hunninghake GW, Kalica AR. Approaches to the treatment of pulmonary fibrosis. *Am J Respir Crit Care Med* 1995; 151: 915–918.
7 Hamilton RF Jr, Thakur SA, Holian A. Silica binding and toxicity in alveolar macrophages. *Free Radic Biol Med 2008; 1*, 44: 1246–1258.
8 Cowan CA, Klimanskaya I, McMahon J, *et al.* Derivation of embryonic stem-cell lines from human blastocysts. *N Engl J Med* 2004; 350: 1353–1356.
9 Isakson BE, Lubman RL, Seedorf GJ, *et al.* Modulation of pulmonary alveolar type II cell phenotype and communication by extracellular matrix and KGF. *Am J Physiol Cell Physiol* 2001; 281: C1291–C1299.
10 Fuchs S, Hollins AJ, Laue M, *et al.* Differentiation of human alveolar epithelial cells in primary culture: morphological characterization and synthesis of caveolin-1 and surfactant protein-C. *Cell Tissue Res* 2003; 311: 31–45.
11 Favia M, Guerra L, Fanelli T, *et al.* Na+/H+ exchanger regulatory factor 1 overexpression-dependent increase of cytoskeleton organization is fundamental in the rescue of F508del cystic fibrosis transmembrane conductance regulator in human airway CFBE41o- cells. *Mol Biol Cell* 2010; 21: 73–86.
12 Spitalieri P, Cortese G, Pietropolli A. Identification of multipotent cytotrophoblast cells from human first trimester chorionic villi. *Cloning Stem Cells* 2009; 11: 535–556.
13 Guerra L, Fanelli T, Favia M, *et al.* Na+/H+ exchanger regulatory factor isoform 1 overexpression modulates cystic fibrosis transmembrane conductance regulator (CFTR) expression and activity in human airway 16HBE14o- cells and rescues DeltaF508 CFTR functional expression in cystic fibrosis cells. *J Biol Chem* 2005; 280: 40925–40933.
14 Taddei A, Folli C, Zegarra-Moran O, *et al.* Altered channel gating mechanism for CFTR inhibition by a high-affinity thiazolidinone blocker. *FEBS Lett* 2004; 558: 52–56.
15 Green RL, Roinestead IC, Boland C, *et al.* Developmental validation of the Quantifiler™ real-time PCR kits for the quantification of human nuclear DNA samples. *J Forensic Sci* 2005; 50: 809–825.
16 Soncini M, Signoroni PB, Bailo M, *et al.* Use of highly sensitive mitochondrial probes to detect microchimerism in xenotransplantation models. *Xenotransplantation* 2006; 13: 80–85.
17 Hsia CC, Hyde DM, Ochs M, *et al.* ATS/ERS Joint Task Force on Quantitative Assessment of Lung Structure. An official research policy statement of the American Thoracic Society/European Respiratory Society: standards for quantitative assessment of lung structure. *Am J Respir Crit Care Med* 2010; 181: 394–418.
18 Ashcroft T, Simpson JM, Timbrell V, *et al.* Simple method of estimating severity of pulmonary fibrosis on a numerical scale. *J Clin Pathol* 1988; 41: 467–470.
19 Moodley YD, Atienza U, Manuelpillai CS, *et al.* Human umbilical cord mesenchymal stem cells reduce fibrosis of bleomycin-induced lung injury. *Am J Pathol* 2009; 175: 303–313.
20 Yue X, Li X, Nguyen HT, *et al.* Transforming growth factor-β1 induces heparan sulfate 6-O-endosulfatase 1 expression *in vitro* and *in vivo*. *J Biol Chem* 2008; 283: 20397–20407.
21 Gomperts BN, Belperio JA, Rao PN, *et al.* Circulating progenitor epithelial cells traffic *via* CXCR4/CXCL12 in response to airway injury. *J Immunol* 2006; 176: 1916–1927.
22 Bossard F, Robay A, Toumaniantz G, *et al.* NHE-RF1 protein rescues ΔF508-CFTR function. *Am J Physiol Lung Cell Mol Physiol* 2007; 292: L1085–L1094.
23 Callis AH, Sohnle PG, Mandel GS, *et al.* Kinetics of inflammatory and fibrotic pulmonary changes in a murine model of silicosis. *J Lab Clin Med* 1985; 105: 547–553.
24 du Bois RM. Strategies for treating idiopathic pulmonary fibrosis. *Nat Rev Drug Discov* 2010; 9: 129–140.
25 Hay J, Shahzeidi S, Laurent G. Mechanisms of bleomycin induced lung damage. *Arch Toxicol* 1991; 65: 81–94.
26 Ortiz LA, Gambelli F, McBride C, *et al.* Mesenchymal stem cell engraftment in lung is enhanced in response to bleomycin exposure and ameliorates its fibrotic effects. *Proc Natl Acad Sci USA* 2003; 100: 8407–8411.
27 Moodley Y, Ilancheran S, Samuel C, *et al.* Human amnion epithelial cell transplantation abrogates lung fibrosis and augments repair. *Am J Respir Crit Care Med* 2010; 182: 643–651.

28 Wang D, Morales JE, Calame DG, *et al.* Transplantation of human embryonic stem cell-derived alveolar epithelial type II cells abrogates acute lung injury in mice. *Mol Ther* 2010; 18: 625–634.
29 Cargnoni AL, Gibelli A, Tosini PB, *et al.* Transplantation of allogeneic and xenogeneic placenta-derived cells reduces bleomycin-induced lung fibrosis. *Cell Transplant* 2009; 18: 405–422.
30 Yildirim AO, Muyal V, John G, *et al.* Palifermin induces alveolar maintenance programs in emphysematous mice. *Am J Respir Crit Care Med* 2010; 181: 705–717.
31 Aguilar S, Scotton CJ, McNulty K, *et al.* Bone marrow stem cells expressing keratinocyte growth factor *via* an inducible lentivirus protects against bleomycin-induced pulmonary fibrosis. *PLoS One* 2009; 4: e8013.
32 Gazdhar A, Fachinger P, van Leer C, *et al.* Gene transfer of hepatocyte growth factor by electroporation reduces bleomycin-induced lung fibrosis. *Am J Physiol Lung Cell Mol Physiol* 2007; 292: L529–L536.
33 Sueblinvong VR, Loi PL, Eisenhauer I, *et al.* Derivation of lung epithelium from human cord blood-derived mesenchymal stem cells. *Am J Respir Crit Care Med* 2008; 177: 701–711.
34 Carraro GL, Perin S, Sedrakyan S, *et al.* Human amniotic fluid stem cells can integrate and differentiate into epithelial lung lineages. *Stem Cells* 2008; 26: 2902–2911.
35 Maron-Gutierrez T, Castiglione RC, Xisto DG, *et al.* Bone marrow-derived mononuclear cell therapy attenuates silica-induced lung fibrosis. *Eur Respir J* 2011; 37: 1217–1225.
36 Lassance RM, Prota LF, Maron-Gutierrez T, *et al.* Intratracheal instillation of bone marrow-derived cell in an experimental model of silicosis. *Respir Physiol Neurobiol* 2009; 169: 227–233.
37 Baritussio A, Bellina L, Carraro R, *et al.* Heterogeneity of alveolar surfactant in the rabbit: composition, morphology, and labelling of subfractions isolated by centrifugation of lung lavage. *Eur J Clin Invest* 1984; 14: 24–29.
38 Fang X, Song Y, Hirsch J. Contribution of CFTR to apical-basolateral fluid transport in cultured human alveolar epithelial type II cells. *Am J Physiol Lung Cell Mol Physiol* 2006; 290: L242–L249.
39 Melloni B, Lesur O, Bouhadiba T, *et al.* Effect of exposure to silica on human alveolar macrophages in supporting growth activity in type II epithelial cells. *Thorax* 1996; 51: 781–786.
40 Haase MG, Klawitter A, Bierhaus A, *et al.* Inactivation of AP1 proteins by a nuclear serine protease precedes the onset of radiation-induced fibrosing alveolitis. *Radiat Res* 2008; 169: 531–542.
41 Davis GS. The pathogenesis of silicosis: state of the art. *Chest* 1986; 89: 166S–169S.
42 Olszewski MA, Huffnagle GB, McDonald RA, *et al.* The role of macrophage in inflammatory protein-1α/CCL3 in regulation of T-cell-mediated immunity to *Cryptococcus neoformans* infection. *J Immunol* 2000; 165: 6429–6436.
43 Li XY, Donaldson K, Brown D, *et al.* The role of tumour necrosis factor in increased airspace epithelial permeability. *Am J Respir Cell Mol Biol* 1995; 13: 185–195.
44 Gosset P, Lassalle P, Vanhée D, *et al.* Production of tumour necrosis factor-α and interleukin-6 by human alveolar macrophages exposed *in vitro* to coal mine dust. *Am J Respir Cell Mol Biol* 1991; 5: 431–436.
45 Driscoll KE, Carter JM, Howard BW, *et al.* Crocidolite activates NF-κB and MIP-2 gene expression in rat alveolar epithelial cells. Role of mitochondrial-derived oxidants. *Environ Health Perspect* 1998; 106: Suppl. 5, 1171–1174.
46 Smith RE, Strieter RM, Phan SH, *et al.* TNF and IL-6 mediate MIP-1α expression in bleomycin-induced lung injury. *J Leukoc Biol* 1998; 64: 528–536.
47 Cutroneo KR. TGF-β-induced fibrosis and SMAD signaling: oligo decoys as natural therapeutics for inhibition of tissue fibrosis and scarring. *Wound Repair Regen* 2007; 15: Suppl. 1, S54–S60.
48 Driscoll B, Buckley S, Bui KC, *et al.* Telomerase in alveolar epithelial development and repair. *Am J Physiol Lung Cell Mol Physiol* 2000; 279: L1191–L1198.
49 Schuyler MR, Gaumer HR, Stankus RP, *et al.* Bronchoalveolar lavage in silicosis. Evidence of type I cell hyperplasia. *Lung* 1980; 157: 95–102.
50 Sisson TH, Mendez M, Choi K, *et al.* Targeted injury of type II alveolar epithelial cells induces pulmonary fibrosis. *Am J Respir Crit Care Med* 2010; 181: 254–263.
51 Chilosi M, Doglioni C, Murer B, *et al.* Epithelial stem cell exhaustion in the pathogenesis of idiopathic pulmonary fibrosis. *Sarcoidosis Vasc Diffuse Lung Dis* 2010; 27: 7–18.
52 Murdoch C. CXCR4: chemokine receptor extraordinaire. *Immunol Rev* 2000; 177: 175–184.
53 Zhao F, Zhang YF, Liu YG, *et al.* Therapeutic effects of bone marrow-derived mesenchymal stem cells engraftment on bleomycin-induced lung injury in rats. *Transplant Proc* 2008; 40: 1700–1705.